



## RESEARCH ARTICLE

# Functional redundancy of the premotor network in hemispherotomy patients

Conrad C. Prillwitz<sup>1</sup>, Bastian David<sup>1</sup> , Gottfried Schlaug<sup>2</sup>, Thomas Deller<sup>3</sup>, Johannes Schramm<sup>4</sup>, Robert Lindenberg<sup>5</sup>, Elke Hattingen<sup>6</sup>, Bernd Weber<sup>7</sup>, Rainer Surges<sup>1</sup>, Christian E. Elger<sup>1</sup> & Theodor Rüber<sup>1,8,9</sup> 

<sup>1</sup>Department of Epileptology, University of Bonn Medical Center, Bonn, Germany

<sup>2</sup>Stroke Recovery Laboratory, Beth Israel Deaconess Medical Center, Harvard Medical School, Boston, Massachusetts

<sup>3</sup>Institute of Clinical Neuroanatomy, Neuroscience Center, Goethe-University Frankfurt, Frankfurt am Main, Germany

<sup>4</sup>Medical Faculty, University of Bonn, Bonn, Germany

<sup>5</sup>Department of History, Philosophy and Ethics of Medicine, Center for Health and Society, Heinrich-Heine-University, Düsseldorf, Germany

<sup>6</sup>Department of Neuroradiology, Goethe-University Frankfurt, Frankfurt am Main, Germany

<sup>7</sup>Institute of Experimental Epileptology and Cognition Research, University of Bonn Medical Center, Bonn, Germany

<sup>8</sup>Department of Neurology, Epilepsy Center Frankfurt Rhine-Main, Goethe-University Frankfurt, Frankfurt am Main, Germany

<sup>9</sup>Center for Personalized Translational Epilepsy Research (CePTER), Goethe-University Frankfurt, Frankfurt am Main, Germany

## Correspondence

Theodor Rüber, Department of Epileptology, University of Bonn Medical Center, Venusberg-Campus 1, 53127 Bonn, Germany. Tel: +49 228 6885 264; Fax: +49 228 6885 261; E-mail: theodor.rueber@ukbonn.de

## Funding Information

This work was supported by grants from the BONFOR research commission of the medical faculty of the University of Bonn (2017-6-02 and 2016-8-07). CCP and BD are recipients of fellowships from *Bischöfliche Studienförderung Cusanuswerk*. TR is supported by the Hessian Ministry of Research and Art's LOEWE initiative. The authors thank Esra Aslim for technical assistance in figure creation. Finally, the authors are grateful for the kind support provided by the Verein zur Förderung der Epilepsieforschung e.V. in Bonn.

Received: 24 June 2021; Accepted: 30 June 2021

*Annals of Clinical and Translational Neurology* 2021; 8(9): 1796–1808

doi: 10.1002/acn3.51427

## Introduction

The human motor system consists of highly integrated cerebral, cerebellar, and spinal populations of neurons forming a complex network to govern voluntary

## Abstract

**Objective:** Using multimodal imaging, we tested the hypothesis that patients after hemispherotomy recruit non-primary motor areas and non-pyramidal descending motor fibers to restore motor function of the impaired limb. **Methods:** Functional and structural MRI data were acquired in a group of 25 patients who had undergone hemispherotomy and in a matched group of healthy controls. Patients' motor impairment was measured using the Fugl-Meyer Motor Assessment. Cortical areas governing upper extremity motor-control were identified by task-based functional MRI. The resulting areas were used as nodes for functional and structural connectivity analyses. **Results:** In hemispherotomy patients, movement of the impaired upper extremity was associated to widespread activation of non-primary premotor areas, whereas movement of the unimpaired one and of the control group related to activations prevalently located in the primary motor cortex (all  $p \leq 0.05$ , FWE-corrected). Non-pyramidal tracts originating in premotor/supplementary motor areas and descending through the pontine tegmentum showed relatively higher structural connectivity in patients ( $p < 0.001$ , FWE-corrected). Significant correlations between structural connectivity and motor impairment were found for non-pyramidal ( $p = 0.023$ , FWE-corrected), but not for pyramidal connections. **Interpretation:** A premotor/supplementary motor network and non-pyramidal fibers seem to mediate motor function in patients after hemispherotomy. In case of hemispheric lesion, the homologous regions in the contralesional hemisphere may not compensate the resulting motor deficit, but the functionally redundant premotor network.

movement.<sup>1</sup> Lesions on all levels of this network can lead to impairments, but compensation might occur through mechanisms of synaptic plasticity, axonal sprouting, and the use of alternate networks.<sup>2</sup> Patients undergoing hemispherotomy for severe and intractable epileptic seizures

are an extreme example for the study of the compensatory capabilities of this network since their large surgical lesion typically makes a residual compensation through the affected hemisphere less likely.<sup>3</sup> Thus, their recovery and restoration of motor function has to be mediated by the intact hemisphere.<sup>4,5</sup> This unique ability to compensate for these large surgical lesions by shifting functions to alternative cortical structures and corticofugal pathways reveals the motor-network's seemingly redundant architecture,<sup>1,6</sup> which seems to be more available as a path of recovery in the developing brain.<sup>7</sup> Different aspects of post-lesional motor network changes have been examined previously, for example, functional MRI (fMRI) studies employing motor tasks that involve movements of the impaired limb,<sup>4,8</sup> as well as structural MRI studies focusing on the integrity of cortico-cortical connections,<sup>9,10</sup> and descending motor pathways.<sup>11–14</sup> While the post-lesional recruitment of non-primary motor areas to enable movements of the impaired limb has been repeatedly observed,<sup>15</sup> the contribution of descending non-pyramidal pathways to motor compensation remains unclear. Based on animal studies in which the pyramidal tract was lesioned,<sup>16,17</sup> a compensatory role of non-pyramidal descending pathways such as the cortico-rubrospinal or cortico-reticulospinal tracts has been postulated.<sup>18,19</sup> In chronic stroke patients, diffusion tensor imaging (DTI) enabled the reconstruction of corticofugal tracts descending through the pontine tegmentum and DTI-derived parameters gave evidence for their contribution to motor recovery.<sup>14,20,21</sup> As previous DTI studies could not specify the anatomical correlates of these tracts with the imaging data available, they were named *alternate Motor Fibers* (aMF). While various reports have confirmed the compensatory role of aMF, their exact role in motor function, their specific anatomical correlates and even their existence in humans is still under debate.<sup>12,22</sup> It has been shown that cortico-rubrospinal and cortico-reticulospinal tracts originate primarily from premotor areas.<sup>6,23</sup> Here, we hypothesized that patients after hemispherotomy might recover their motor function through recruitment of cortical motor areas rostral to M1 (i.e., premotor cortex) in the contralesional hemisphere and that these areas exert their effects on motor output through fibers in non-pyramidal descending pathways governing voluntary movement of the impaired extremity. Twenty-five hemispherotomy patients underwent functional and structural MRI and we performed three consecutive steps to test this hypothesis: First, patients underwent task-based functional MRI (fMRI) to identify areas being active during movements of the affected and the non-affected hand. Second, resulting areas of activation were used as nodes for a cortical analysis of structural and functional connectivity. Third, brainstem nodes

were defined for an additional structural connectivity study of descending pathways in this restored network model.

## Subjects and Methods

### Study subjects

Our initial sample included 34 patients who had undergone transsylvian functional hemispherotomy<sup>24</sup> for severe pharmacoresistant epilepsy between 1992 and 2012 (except for one patient who underwent hemispherotomy before 1992). Data were acquired between 2011 and 2014. Patients included in the present analysis had to have an ability to undergo 2 h of structural and functional MR-scans, in addition to several hours of language and motor testing over two consecutive days. Nine of those initial 34 patients were not able to complete the entire imaging protocol (see below) and were excluded from the current analysis resulting in a final group of 25 hemispherotomy patients (13 women; mean age at scan  $\pm$  SD:  $22.8 \pm 8.5$  years; mean age at surgery  $\pm$  SD:  $12.5 \pm 8.2$ ). Some other details of this group were previously published.<sup>3,14</sup> Underlying pathologies were grouped into the categories “vascular” (such as perinatal strokes or hemorrhages resulting in porencephaly), “developmental” (such as hemimegalencephaly, Sturge-Weber syndrome or polymicrogyria), and “progressive” (Rasmussen encephalitis) according to our previous study.<sup>14</sup> All patients received physiotherapy, occupational therapy, and logotherapy as part of their early rehabilitation training already in the hospital. There were then admitted to certified neurorehabilitation centers, where they underwent specialized neuropsychiatric rehabilitation for on average 6 to 8 weeks. Patients were included on average 124.16 months after surgery in this study (see Table 1 for patient characteristics). Twenty-four subjects (12 women; mean age  $\pm$  SD:  $31.5 \pm 12.3$  years) without a history of neurological or psychiatric disorders were included as a control group. The study was approved by the local Institutional Review Board and all participants/their legal guardians gave written informed consent. The difference in mean age between the patients and the control group is due to our local IRB allowing the inclusion of minor patients, since their imaging data could be used on clinical grounds, but objecting the inclusion of minor healthy control subjects in our study. We have added “age at scan” as a covariate to statistical analyses conducted (see below).

### Functional motor assessment

Each patient underwent the Upper Extremity Fugl-Meyer Score<sup>25</sup> (FM-UE) to quantify motor impairment (FM-UE\_motor) and sensation (FM-UE\_sensory) of the

**Table 1.** Clinical characteristics of the patient group.

ID	Lesionside	Gender	Etiology	Age at surgery [years]	Age at scan [years]	Surgery–scan–interval [months]	Total Fugl-Meyer/sub-scores		
							Total FM-UE* [max 126]	FM-UE_motor [max 56]	FM-UE_sensory [max 12]
<b>Patients</b>									
1	L	M	Porencephaly	11	17	68	83	32	7
2	L	M	Encephalitis	19	20	14	67	20	6
3	R	M	Porencephaly	17	20	36	67	15	9
4	L	F	Encephalitis	18	21	26	62	15	5
5	R	M	Porencephaly	15	18	27	78	25	7
6	R	F	Encephalitis	31	46	182	68	18	8
7	L	F	HMEG	6	25	232	95	36	10
8	L	F	Porencephaly	14	21	91	81	24	8
9	L	F	Porencephaly	19	21	24	71	26	3
10	L	F	HMEG	4 m	18	216	78	25	9
11	R	M	Polymicrogyria	10	24	162	74	18	10
12	R	F	HMEG	1	12	131	106	46	11
13	L	F	Encephalitis	7	44	438	71	17	7
14	L	F	Porencephaly	10	20	124	92	32	11
15	L	F	Porencephaly	12	23	132	81	25	8
16	R	F	Porencephaly	11	21	126	75	24	7
17	L	M	Encephalitis	13	18	70	72	20	6
18	L	M	Porencephaly	11	19	96	90	35	10
19	R	F	Encephalitis	7	12	65	105	47	7
20	R	F	Porencephaly	25	36	130	53	13	2
21	R	F	HMEG	1	16	189	77	24	7
22	R	F	Porencephaly	16	27	131	58	14	5
23	R	M	SWS	2	20	222	90	38	7
24	R	M	Encephalitis	29	33	45	58	14	4
25	L	F	Porencephaly	9	20	127	77	27	7
Mean ± SD	16 left	13 female		12.5 ± 8.2	22.8 ± 8.5	124.2 ± 92.2	77.2 ± 13.7	25.2 ± 9.6	7.2 ± 2.3
<b>Controls</b>									
1		m			44				
2		m			18				
3		f			27				
4		m			30				
5		m			22				
6		f			22				
7		m			23				
8		f			22				
9		f			21				
10		f			20				
11		f			49				
12		f			50				
13		m			53				
14		f			25				
15		f			22				
16		f			28				
17		m			33				
18		m			34				
19		m			58				
20		f			48				
21		f			19				

(Continued)

**Table 1** Continued.

ID	Lesionside	Gender	Etiology	Age at surgery [years]	Age at scan [years]	Surgery–scan–interval [months]	Total Fugl-Meyer/sub-scores		
							Total FM-UE* [max 126]	FM-UE_motor [max 56]	FM-UE_sensory [max 12]
22		m			35				
23		m			31				
24		m			21				
Mean ± SD		12 female			31.5 ± 12.3				

Abbreviations: F, female; FM-UE\_motor, Fugl-Meyer motor score of the upper extremity (maximum = 56); FM-UE\_sensory, Fugl-Meyer sensory score of the upper extremity (maximum = 12); HMEG, Hemimegalencephaly; L, left; M, male; R, right; SD, standard deviation; SWS, Sturge-Weber syndrome; Total FM-UE, Fugl-Meyer score of the upper extremity (maximum = 126).

impaired upper extremity among other motor tests. As in a previous study,<sup>14</sup> reflex activity and coordination/speed were excluded from the FM-UE\_motor subscore, since the focus of our study were corticospinal networks, which we supposed to be more clearly associated with voluntary motor tasks and which were also tested in the fMRI-paradigm (see below). (See Fig. 1 for more detail about the subdivision of the FM-UE score and Table 1 for individual patient scores.)

### Analysis of clinical explanatory variables of motor impairment

To identify relevant clinical explanatory variables of FM-UE\_motor, a stepwise regression analysis using *Stata/IC 14.2* (*StataCorp*) was performed among the following previously identified factors that might have an effect on recovery

of motor function: *age at surgery*, *age at scan*, *gender (female, male)*, *affected hemisphere (right, left)*, and *etiology (vascular, developmental, progressive)*. Statistical significance was determined as  $p \leq 0.05$ , and estimator's robustness were confirmed using bootstrapping (10,000 repetitions) initiated by a randomly but reproducible set seed.

### Image acquisition

A 3T MAGNETOM Trio scanner (Siemens Healthineers, Erlangen, Germany) was used to acquire structural and functional magnetic resonance imaging sequences. The protocol included 3D T1- and T2-weighted scans, resting-state fMRI, task-related fMRI, and diffusion tensor imaging (DTI). First, a 3D T1-weighted (resolution =  $1.0 \times 1.0 \times 1.0 \text{ mm}^3$ , TR = 1570 msec, TE = 3.42 msec, flip angle =  $15^\circ$ ) and a 3D T2-weighted scan (resolution =  $1.0 \times 1.0 \times 1.0 \text{ mm}^3$ ,

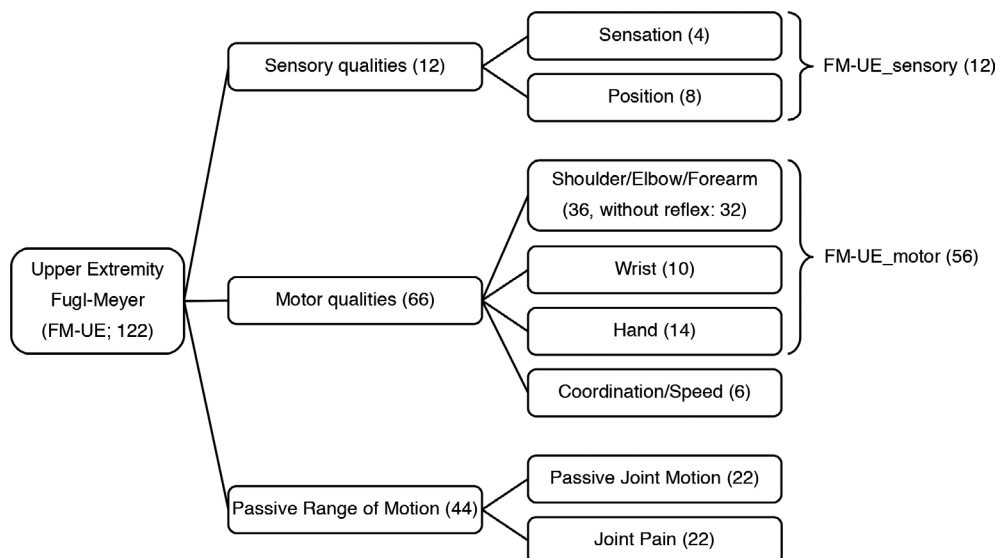


**Figure 1.** Subdivisions of the Upper Extremity Fugl-Meyer Score (FM-UE). Maximum scores for each sub-score are provided in parentheses. FM-UE\_motor, Fugl-Meyer motor score of the upper extremity; FM-UE\_sensory, Fugl-Meyer sensory score of the upper extremity.

TR = 3200 msec, TE = 455 msec, flip angle = 120°) were obtained. Subsequently, subjects were scanned while at rest (resolution = 3.0 × 3.0 × 3.3 mm<sup>3</sup>, TR = 2500 msec, TE = 30 msec, flip angle = 90°, 240 volumes) and while performing a motor-task (resolution = 3.0 × 3.0 × 3.3 mm<sup>3</sup>, TR = 3000 msec, TE = 35 msec, flip angle = 90°, 140 volumes). For resting-state fMRI, subjects were instructed to lie still and fixate a crosshair without thinking on something particular or falling asleep. If a subject fell asleep or closed their eyes during resting-state fMRI, the sequence was aborted and restarted a maximum of two times. During the following task-related fMRI study, subjects were instructed to repeatedly move the most distal movable joint of their impaired upper extremity with a frequency of 2 Hz for 30 sec: Either subjects should repeatedly tap the thumb and middle finger, or they should repeatedly move the hand or the forearm. The experiment was set up as a block design with interleaving periods of rest of the same duration. Movements were trained before entering the scanner room and an observer was present in the scanner room during all fMRI measurements to ensure correct execution of the tasks. If the motor task was not properly conducted (including mirror movements of the unimpaired hand), the task-based motor fMRI sequence was aborted and restarted a second and a third time. The scan session was aborted and the patient was

excluded from the study if the motor task could not be properly conducted at the third attempt. Before acquisition of DTI, a 10-min break was taken for patients to rest outside of the scanner. DTI was performed using a single shot, dual echo, spin-echo, echo planar imaging sequence (resolution = 1.72 × 1.72 × 1.7 mm<sup>3</sup>, TR = 12000 msec, TE = 100 msec, flip angle = 90°) with 60 directions and a *b*-value of 1000 s/mm<sup>2</sup> as well as six baseline volumes with a *b*-value of 0 s/mm<sup>2</sup>. The scanning protocol of the healthy control subjects was the same as for the patients. All control subjects performed the motor task with either hand separately.

### General preprocessing

We first delineated surface representations from T1-weighted images to provide an anatomical framework as part of the general preprocessing. In the following multimodal analysis, we (1) analyzed task-based fMRI data to identify cortical areas involved in the movement of patient's impaired and unimpaired hands, (2) used the cortical areas as nodes for a functional connectivity analysis, and (3) defined additional brainstem nodes based on anatomical knowledge for a final structural connectivity analysis. These procedures are explained in detail in the following section (and depicted schematically in Fig. 2).

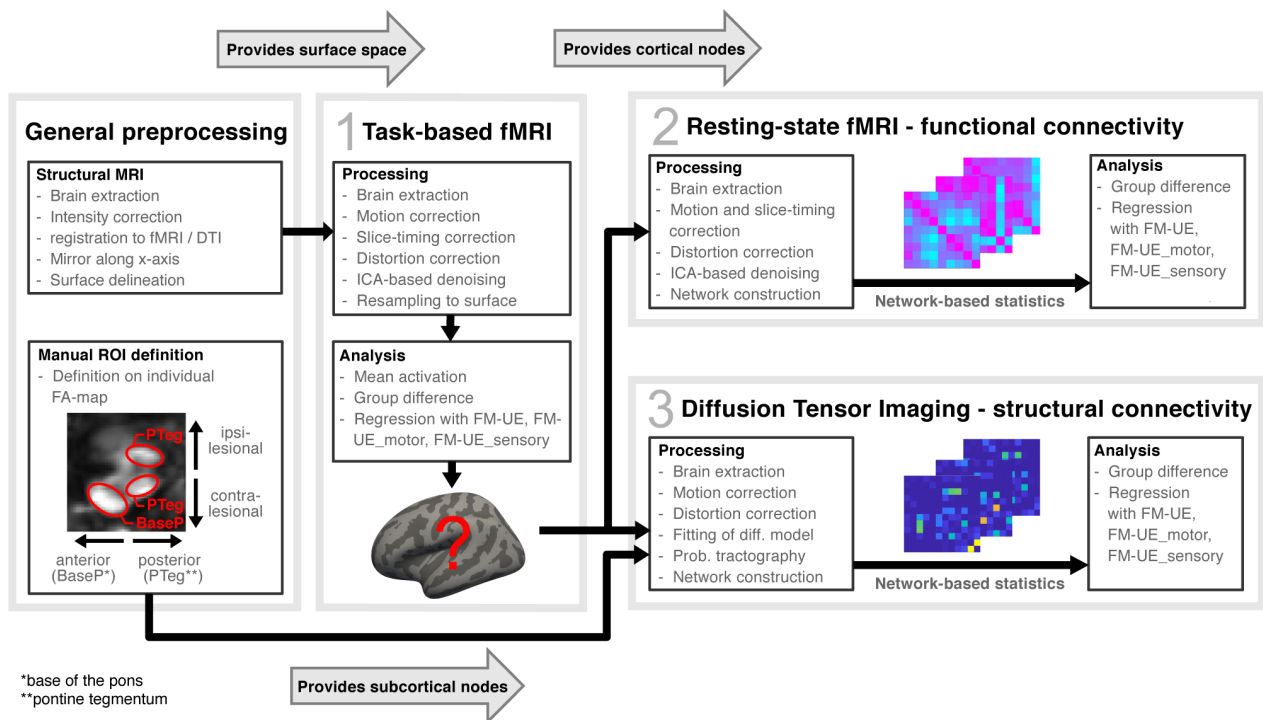


**Figure 2.** Schematic of the 3 consecutive steps of imaging analysis applied. FA-map, Fractional anisotropy map; FM-UE\_motor, Fugl-Meyer motor score of the upper extremity; FM-UE\_sensory, Fugl-Meyer sensory score of the upper extremity; ICA-based denoising, independent component analysis-based denoising.

Structural and functional data were preprocessed based on the Human Connectome Project's minimal preprocessing pipeline.<sup>26</sup> Briefly, non-brain tissue of T1-weighted scans was removed prior to intensity inhomogeneity correction using FMRIB's Software Library (FSL) 5.0 ([www.fmrib.ox.ac.uk/fsl](http://www.fmrib.ox.ac.uk/fsl)).<sup>27</sup> Due to the vulnerability of global surface delineation to local anatomical defects as found in the lesional hemisphere of patients after hemispherotomy, contralesional hemispheres were mirrored along the x-axis to eliminate those defects from the data. The resulting symmetric brains consisting of two contralesional hemispheres were passed. The T1-derived surfaces were registered to the symmetric *fsaverage-sym* template to enable comparison of originally left- as well as right-sided hemispheres.<sup>29</sup> After modality-specific preprocessing steps were completed (see below), DTI and fMRI data were registered to their respective T1-weighted volume using boundary-based registration and subsequently projected on the *fsaverage-sym* surface template. All previously described processing steps were visually inspected for accuracy by a neuroradiologically trained rater and manually corrected if necessary.

1 Motor fMRI: Motor fMRI data were analyzed using FSL Feat<sup>27</sup> and Freesurfer<sup>28</sup> for surface-based analysis. Surface-based analysis of fMRI data allows for a more fine-grained distinction between activation in adjacent cortical areas as it allows smoothing of time-series data based on Geodesic rather than Euclidean distance. This is crucial to distinguish between activation clusters in primary and non-primary motor and sensory areas. After removal of non-brain tissue, all data were corrected for motion and slice timing. As EPI-Sequences suffer from significant susceptibility induced distortions, the Tolerable Obsessive Registration and Tensor Optimization Indolent Software Ensemble (TORTOISE) was used to correct those by means of constrained registration.<sup>30</sup> While most patients showed increased head-motion during movement of the impaired limb, absolute and relative displacement of volumes were smaller than 1.5 mm and thus considered acceptable. To address the motor task-related noise within the BOLD-signal, data were decomposed by means of independent component analysis (ICA) and manually classified in signal and noise components following established routines.<sup>31</sup> Noise components were partially regressed out of the data and the denoised data were projected onto the individual surface representation derived from the T1-weighted images and smoothed by a 5-mm Gaussian kernel for all subsequent analysis. A vertex-wise general linear model (GLM) was applied using the PALM software package<sup>32</sup> and nonparametric permutation inference to find clusters being active during the

movement of impaired and unimpaired hands in patients as well as for movement of the left and right hand in controls. All permutation tests were run with 10,000 repetitions and results were family-wise error (FWE) corrected for multiple comparisons by means of threshold-free cluster enhancement.<sup>33</sup>

- 2 Resting-state fMRI: Resting-state fMRI data were brain-extracted and motion corrected prior to slice-timing correction, susceptibility induced distortion correction, and ICA-based denoising as described in 1. Suprathreshold clusters ( $p \leq 0.05$ , FWE-corrected) indicating group-level activation during the movement of patients' impaired and unimpaired hand as described in 1 were binarized and projected from the inflated gray matter surface into the cortical ribbon. The resulting  $n$  volumetric regions of interest (ROI) were used as nodes to read out the mean time series from the resting-state data. Individual  $n \times n$  adjacency matrices were constructed by computing the full correlation coefficient between the time series data of all node pairs. Network-based statistics<sup>34</sup> (NBS) were used to identify differences between the functional connectivity profile of patients and controls and to find specific sub-networks associated with sensory and/or motor function within the patient group. NBS is a power-full method to control the FWE when performing mass univariate testing on network data and can be thought of as an application of conventional cluster statistics<sup>35</sup> to a graph.<sup>34</sup> All tests were conducted with an initial network forming threshold of 3.1 and 10,000 permutations.
- 3 Diffusion tensor MRI: DTI datasets were brain extracted and realigned to the mean of the b0 images to address motion artifacts before correcting for eddy current-induced artifacts and susceptibility-induced distortions as described in 1. A probabilistic diffusion model was fitted on the data by using FSL's BEDPOSTX modeling crossing fibers using Markov Chain Monte Carlo sampling and diffusion tensors were derived for each voxel by using FSL's DTIFIT.<sup>36</sup> For probabilistic tractography of the motor network, the cortical ROIs were obtained by projecting the group level activation clusters derived from the patient's task-based fMRI analysis as described in 1 into the individual patient or control diffusion space. As fMRI activation clusters are located within the cortical ribbon, but the definition of tractography seeds within gray matter is problematic, all ROIs were projected into the juxtacortical white matter. This allowed us to benefit from group-level defined ROIs while taking subject-specific gyral patterns into account. Additionally to the cortical/juxtacortical nodes defined by motor task-based fMRI, five pontine/mesencephalic ROIs were manually defined for each patient and for each of the controls' hemispheres. ROI delineation was visually guided by intensity differences on the FA map as well as by

color-coded diffusion directions of the overlaid principal vector map in the subject's individual diffusion space. Pontine/mesencephalic ROIs included both ipsi- and contralesional red nuclei (RN), for analysis of cortico-rubral connectivity. An ROI within the contralesional base of the pons (BaseP) was defined to perform tractography of the pyramidal tract. Due to tract degeneration, it was not possible to delineate an ROI in the ipsilesional BaseP. Finally, ipsi- and contralesional ROIs within the pontine tegmentum (PTeg) were delineated to reconstruct aMF. Adjacency matrices representing structural connectivity in each subject were constructed by computing the streamline-count between all pairs of ROIs. Statistical analysis was conducted as described in 2.

All analyses of functional and structural connectivity were equally controlled for age at scan and gender and, when FM-UE\_motor was subjected to regression analyses, FM-UE\_sensory was included as a covariate as well.

## Results

### Clinical explanatory variables of FM-UE scores

As reported in our previous publication,<sup>3,14</sup> the stepwise regression analysis showed *age at surgery* to be the only statistically significant ( $p < 0.001$ ) explanatory variable for FM-UE\_motor. All other explanatory variables did not reach significance [*age at scan* ( $p = 0.881$ ), *affected hemisphere* ( $p = 0.822$ ), *etiology* ( $p = 0.887$ ), *gender* ( $p = 0.93$ )], and were consequently removed from the model. Bootstrapping confirmed high reproducibility (*age at surgery*,  $p < 0.001$ ) and suggested the inclusion of *age at surgery* for further regression analyses. A consecutive simple regression analysis also confirmed *age at surgery* as an explanatory variable of FM-UE\_motor ( $p < 0.001$ ), with an  $R^2$  of 0.41: the younger the patient was at surgery, the less likely he or she showed motor impairment later.

### Imaging explanatory variables of FM-UE scores

Seven of the initial 34 patients failed to correctly execute the motor task thrice and were excluded. Two different patients could not complete the DTI acquisition due to discomfort resulting in a total of nine patients who were excluded from the study. Of the 25 remaining patients, three patients could tap the thumb and the middle finger as requested, 16 patients had to move their hand instead, and six patients had to move the forearm. Eleven patients needed a second attempt for the motor task and four patients needed a third attempt. Seven patients fell asleep

during the acquisition of the resting-state fMRI, six patients needed a second attempt after having taken a break, and one patient needed a third attempt to complete the resting-state fMRI while being awake.

- 1 *Motor fMRI*: Clusters representing mean activation during movement of patients' impaired limb (finger, hand, or forearm) were found within the supplementary motor area (SMA), premotor area (PMA), inferior frontal gyrus (IFG), as well as the superior (SPL) and inferior parietal lobe (IPL, all  $p \leq 0.05$ , FWE-corrected, see Fig. 3A). Movement of the unimpaired limb resulted in activation within the primary motor cortex (M1) and the primary somatosensory cortex (S1), similar to the activation seen within the control group (all  $p \leq 0.05$ , FWE-corrected, see Fig. 3B and C). No activation in the hemisphere ipsilateral to the limb moved was found in the control group. The additional regression analysis with functional measures within the patient group yielded no significant results.
- 2 *Resting-state fMRI*: Differences in functional connectivity between patients and controls were found for the connection M1–SMA, which was stronger in patients ( $p = 0.048$ , FWE-corrected). The opposite contrast, testing for stronger connections in controls as compared to patients, yielded no significant results. Regression analysis revealed a positive correlation between FM-UE\_sensory and the functional connectivity within the subnetwork consisting of S1–IFG, IFG–SPL, and SPL–IPL ( $p = 0.03$ , FWE-corrected). Regression analyses with FM-UE and FM-UE\_motor yielded non-significant results (see Fig. 4 for details).
- 3 *Diffusion MRI*: Group-differences in structural connectivity were found for a subnetwork consisting of the connections SMA–contralesional-RN (i.e., cortico-rubral connection/aMF), SMA–contralesional-BaseP (i.e., pyramidal tract), SMA–contralesional-PTeg (i.e., aMF), and SMA–ipsilesional-PTeg (i.e., aMF), which showed a significantly stronger connectivity in patients as compared to controls ( $p < 0.001$ , FWE-corrected). The opposite contrast indicated weaker connections within the cortical sub-network SPL–M1–IPL in patients as compared to controls ( $p = 0.002$ , FWE-corrected). A regression analysis showed a significant positive correlation between FM-UE\_motor and structural connectivity of the subnetwork M1–SMA–ipsilesional-PTeg ( $p = 0.023$ , FWE-corrected). No structural connection was found to correlate with FM-UE\_sensory (see Fig. 4 for details).

## Discussion

In the present study we have tested the hypothesis that patients after hemispherotomy recruit cortical motor

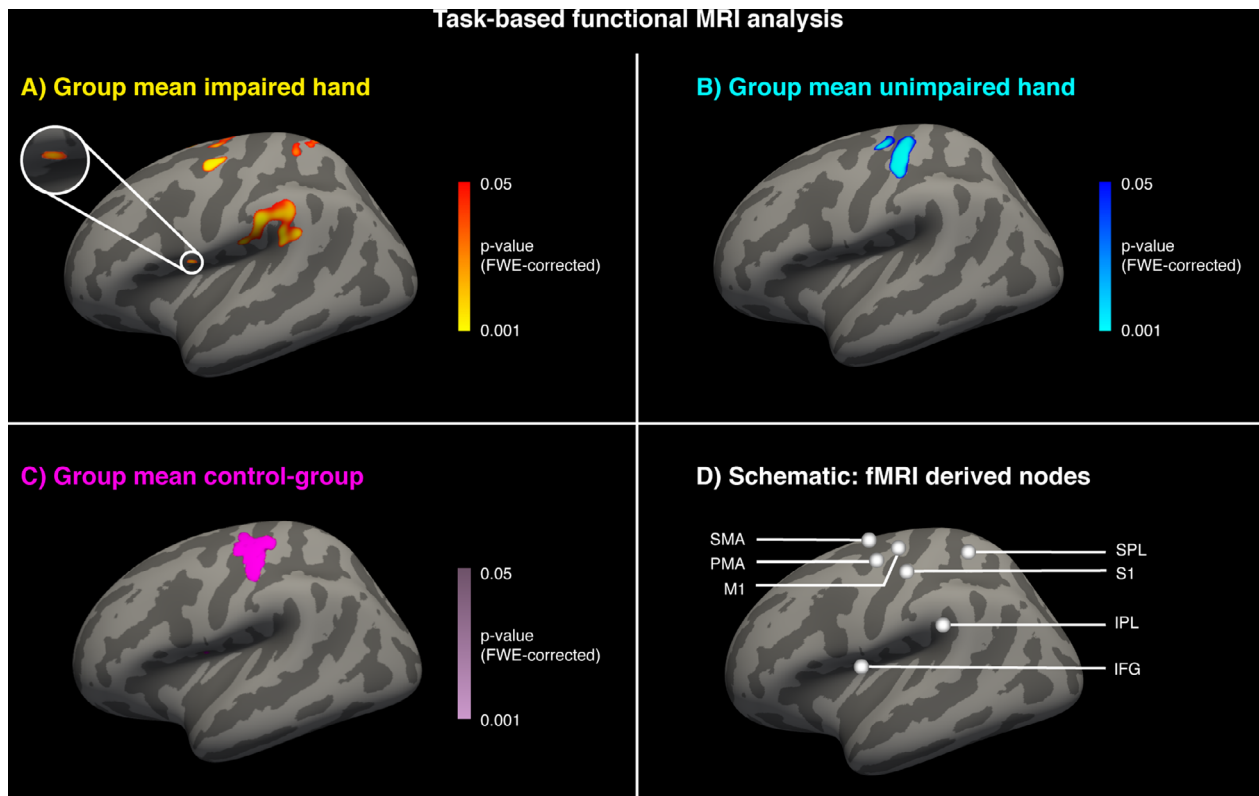


**Figure 3.** Results of motor task-based functional MRI analysis. Mean activation during movement of the impaired hand (A) and the unimpaired hand (B) in the patients' group and mean activation of both hands in the control group (C). All results were family-wise error-corrected (FWE-corrected) by means of threshold-free cluster enhancement. IFG, Inferior Frontal Gyrus; IPL, Inferior Parietal Lobe; M1, Primary Motor Cortex; PMA, Premotor Area; S1, Primary Somatosensory Cortex; SMA, Supplementary Motor Area; SPL, Superior Parietal Lobe.

areas rostral to M1 in the contralesional hemisphere for voluntary movements of the impaired extremity and that the output of these areas contribute to non-pyramidal descending pathways mediating motor recovery. Our main findings can be summarized as follows: Premotor/supplementary motor areas show widespread activation, while M1 is not active during movement of patient's impaired hand. Descending tracts originating in the SMA show a higher structural connectivity in patients as compared to controls. Tracts showing a significant correlation with the degree of motor impairment originate in M1 and SMA, descend through the ipsilesional pontine tegmentum and correspond to aMF. No correlation with motor impairment was found for the pyramidal tract.

For the study of motor recovery, patients after hemispherotomy are of paramount interest. The procedure of hemispherotomy leaves the contralesional hemisphere as the only possible mediator of motor recovery. Motor recovery after hemispherotomy, thus, entails the concept that one hemisphere can compensate for the other.<sup>5</sup> More importantly, brain lesions leading to hemispherotomy and hemispherotomy itself typically occur during infancy or

early childhood, when the brain is not fully matured and thought to be most plastic. Indeed, several studies have shown how early lesions facilitate motor recovery.<sup>12,37</sup> Küpper and colleagues observed grasping ability after hemispherotomy only in patients with pre- or perinatal lesions.<sup>12</sup> The pyramidal tract is bilaterally organized at birth, but uncrossed connections are pruned around the age of one and a half years in normal development. Lesions occurring earlier to the motor system lead to the preservation of these normally transient ipsilateral connections, which can then be reinforced for motor recovery<sup>7</sup> and may mediate distal movements.<sup>14</sup> Whereas in our study, no significant effect of etiology (*vascular|developmental|progressive disorders*) on FM-UE\_motor could be observed, *age at surgery* could explain FM-UE\_motor. The reason for the non-significance of *etiology* most likely lies in the broad three-tier classification (*vascular|developmental|progressive disorders*) and the considerable variance of age of lesion/the different patient histories within the classes, which cannot be clearly determined for individual patients.<sup>14</sup> While for the patients with neurodevelopmental disorders, their fetal onset is subject to informed



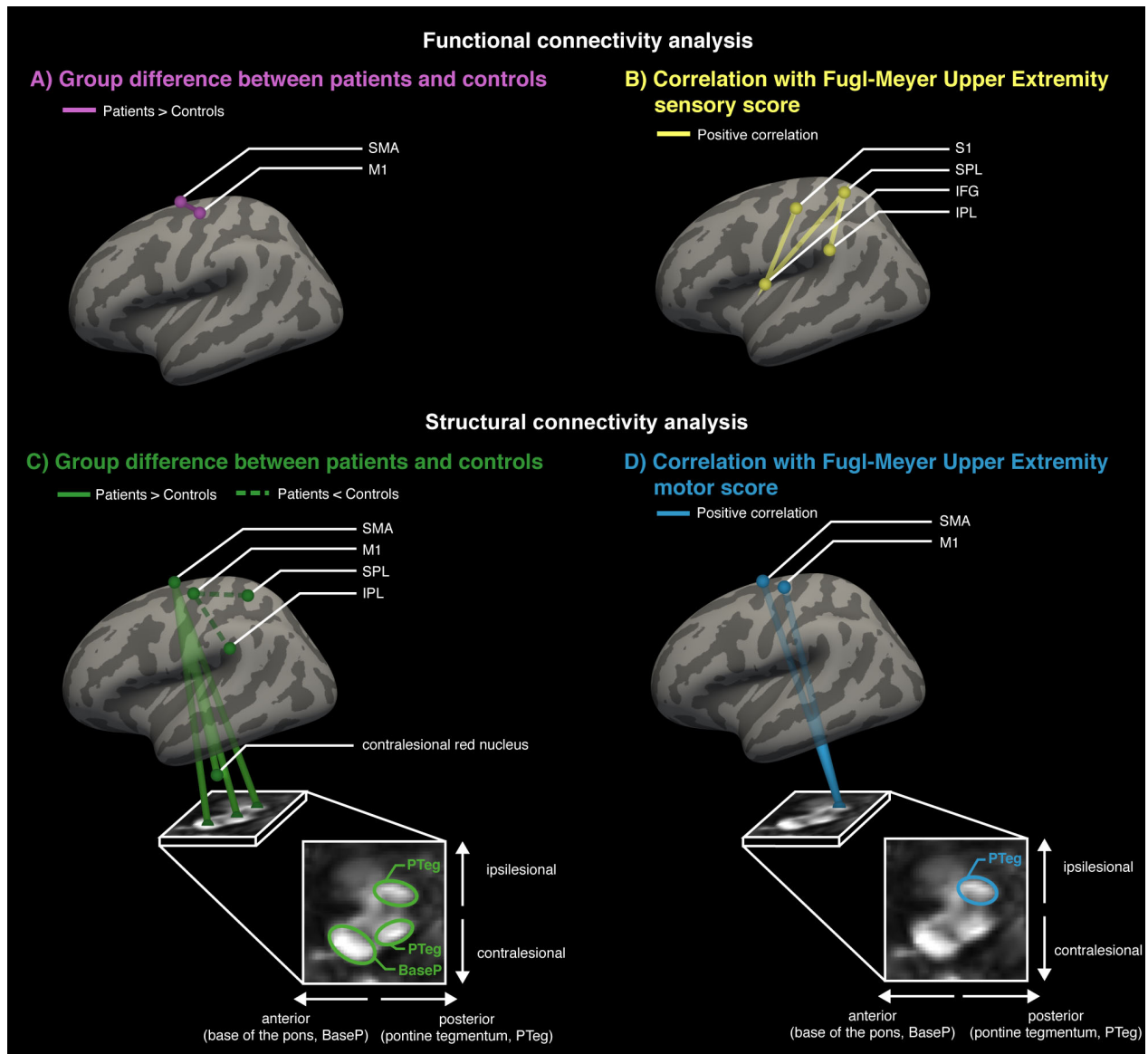


**Figure 4.** Results of functional (A and B) and structural (C and D) connectivity analyses. (A) Functional connectivity group difference indicating stronger connections between SMA and M1 in patients as compared to controls ( $p = 0.048$ , FWE-corrected). (B) Functional connectivity sub-network correlating with the FM-UE\_sensory subscore ( $p = 0.03$ , FWE-corrected). (C) Structural connectivity differences between patients and controls. (D) Structural connectivity network correlating with the FM-UE\_motor sub-score controlled for FM-UE\_sensory. All analysis A–D were additionally corrected for age and gender. All cortical nodes are defined by the results of the fMRI analysis shown in Figure 3. All pontine/mesencephalic nodes were manually defined (see body of the manuscript). BaseP, Base of the Pons; IFG, Inferior Frontal Gyrus; IPL, Inferior Parietal Lobe; M1, Primary Motor Cortex; S1, Primary Somatosensory Cortex; SMA, Supplementary Motor Area; SPL, Superior Parietal Lobe; PTeg, Pontine tegmentum.

speculation, the lesions of patients with vascular pathologies may be dated to the late third trimester (later than 36 weeks) or the first 6 months after birth.<sup>38</sup> Patients in this group suffered from Rasmussen’s Encephalitis, which is known to have a median onset age of 6 years.<sup>39</sup> Unsurprisingly, *age at surgery* varies between patient subgroups (*developmental < vascular < progressive disorders*), as

children with brain lesions occurring earlier in the lifespan are more likely to undergo hemispherotomy earlier. It may, thus, be discussed to what degree the significant effect of *age at surgery* on FM-UE\_motor represents a surrogate marker for *age of lesion* or as to what extent hemispherotomy itself is a stimulus for neuroplastic reorganization (presuming that earlier hemispherotomy

occurs to a more plastic brain) in addition to the underlying lesion. Regardless of whether the hemispherotomy as such or the lesion leading to hemispherotomy triggers neuroplastic remodeling, for the study it is important to note that the surgery–scan interval is sufficiently long (between 14 and 438 months, in average 124 months; see Table 1) for the patients to reach a static plateau phase of motor recovery. While the heterogeneity of the hemispherotomy cohort and the possible effects of two plastic stimuli (discussed above) complicate the development of a general timeline for motor recovery after hemispherotomy, in stroke recovery research, 6 months are seen as the subacute phase in which most the patients' motor recovery potential is exploited.<sup>40</sup> The results of the current study speak in favor of our hypothesis that in the postoperative brain premotor/supplementary motor areas giving origin to aMF are recruited as an alternate system to functionally compensate the motor deficit. aMF are thought to be the tractography correlate of the cortico-rubrospinal and cortico-reticulospinal tracts and have been subject to several DTI studies investigating motor recovery. However, legitimate skepticism has been fostered as to whether cortico-rubrospinal and cortico-reticulospinal tracts do exist in humans and as to whether sensory fibers constitute the neuroanatomical underpinning of aMF instead of motor fibers.<sup>22</sup> Indeed, the characterization of aMF has relied less on their anatomical trajectory and more on their functional relevance as indicated by observed relations between diffusivity parameters and motor function. A long-standing problem of aMF-studies is that M1 is used as ROI for the reconstruction of aMF by means of tractography. Tracer studies in animals, however, have proven a premotor origin of cortico-rubral and cortico-reticular connections<sup>23</sup> and also a DTI study has shown how aMF emanate from premotor areas.<sup>41,42</sup> Our study is, thus, the first to investigate structural connectivity of aMF using cortical seed regions not defined by anatomical landmarks, but by fMRI. It thereby links cortical premotor areas to aMF and suggests both as network alternative to the pyramidal system in the lesioned brain. While their rudimentary bihemispheric organization allows other systems, such as the language and the swallowing system to rely on the built-in redundancy of the other hemisphere,<sup>43,44</sup> this does not seem to be the case for the motor system. Like most complex biological systems, the brain shares the trait of degeneracy, which is defined as “the ability of elements that are structurally different to perform the same function or yield the same output”.<sup>45</sup> The premotor network may well be termed a *degenerate/functionally redundant* (instead of structurally redundant) motor system, as it is structurally different to M1, but seems to show functional redundancy in the lesioned brain and is functionally distinct in the

healthy brain. The importance of the SMA is underlined by the observation that the structural/functional connectivity of five inputs/outputs of the SMA show between-group differences, whereas only one input/output of the M1 shows statistically significant differences between patients and controls. The neuroanatomical underpinnings of the connections reconstructed remain at least partly subject to speculation. The higher functional connectivity between M1 and SMA may be seen as a possible prerequisite for re-mapping. The cortical connections to the pons most likely correspond to corticospinal fibers (connections to base of the pons) and aMF (connections to pontine tegmentum). The cortical connections to the ipsilesional (!) pontine tegmentum are interesting as there are several animal studies investigating reinnervation after hemidecortication or pyramidotomy which found sprouting of crossing fibers targeting the ipsilesional red nucleus.<sup>17,46</sup> Rubrospinal output fibers from the magnocellular part of the red nucleus also cross the midline (decussation of Forel) and may, thus, exert control over the contralesional/impaired side where they have been hypothesized to make connections with alpha-motoneurons.<sup>47</sup> The crossing of rubrospinal (!) fibers from the magnocellular part of the red nucleus, however, cannot be visualized as the caudal extension of anatomy covered by DTI volumes is limited. (Fig. 5 provides a synopsis of our results.)

There are several caveats to bear in mind when interpreting the results of our study: The cross-sectional nature of our study design makes it more difficult to determine whether the structural alterations found are not only epiphenomenal, but the result of preceding plastic remodeling mediating functional compensation. Furthermore, the differing degree of motor recovery in hemispherotomy patients has prevented our subjects to conduct a consistent motor task for the fMRI; not all patients were equally able to tap their fingers or move their wrist. This is especially relevant as proximal movements are more bilaterally and more anteriorly represented<sup>48</sup> and as motor imagery is thought to activate premotor and particularly supplementary motor areas.<sup>49</sup> Additionally, no electrophysiological measures for mirror movements were employed and isometric mirror contractions may have been missed. However, the observed relation between connectivity indices of connections originating in these regions and motor function are indicative of their functional relevance. Lastly, it should be noted that the reflex activity section and the coordination/speed section were excluded from the standardized Fugl-Meyer test and that the test scores are, thus, not comparable to other studies.

It is our hope that this study will contribute to our nascent understanding of motor recovery after hemispheric lesions. The great variation of patient histories leading to

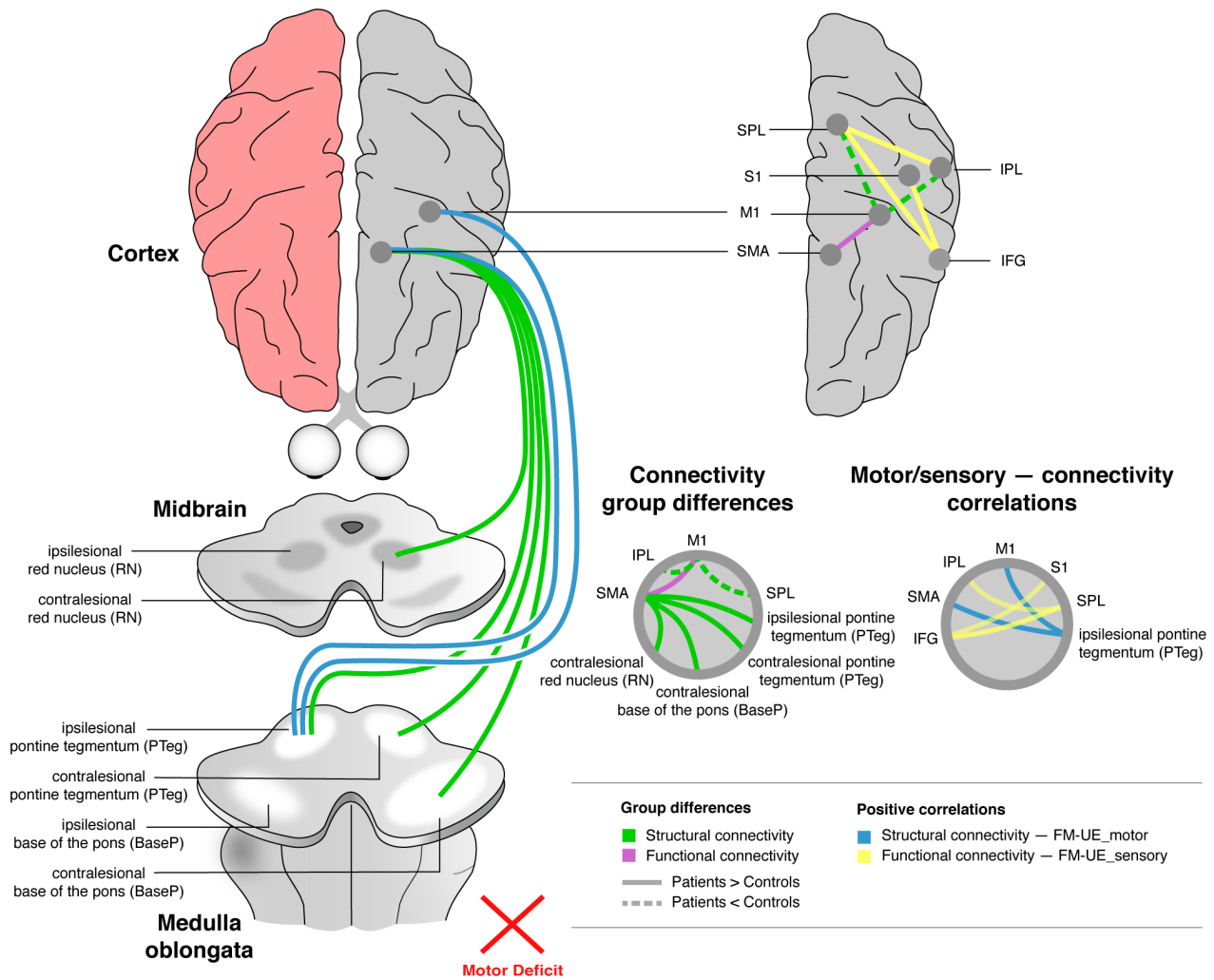


**Figure 5.** Schematic of functional and structural connectivity analysis results. FM-UE\_motor, Fugl-Meyer motor score of the upper extremity; FM-UE\_sensory, Fugl-Meyer sensory score of the upper extremity; IFG, Inferior Frontal Gyrus; IPL, Inferior Parietal Lobe; M1, Primary Motor Cortex; SMA, Supplementary Motor Area; S1, Primary Sensory Cortex; SPL, Superior Parietal Lobe.

hemispherotomy and the relatively low numbers are the most important limitation of this study. This weakens not only the statistical power of analyses run (such as the step-wise regression analysis), but complicates the search for the brain’s compensatory strategies after hemispheric lesions. Importantly, would like to assert that for this reason it has never been the aspiration of the current study to establish a generally applicable rule for the description or prediction of motor recovery in hemispherotomy/hemispherectomy patients, but to showcase the maximal adaptive potential of the motor system and highlight its mechanism of recovery. As mentioned above, in hemispherotomy patients, a maximally invasive lesion occurs to a brain in a period, where it is thought to be maximally plastic. Our better understanding of the mechanism of this unparalleled neuroplastic reorganization that we witness in our patients may inspire

new rehabilitative therapies harnessing the functional redundancy/degeneracy of the premotor/supplementary motor network.

### Acknowledgment

This work was supported by grants from the BONFOR research commission of the medical faculty of the University of Bonn (2017-6-02 and 2016-8-07). CCP and BD are recipients of fellowships from *Bischöfliche Studienförderung Cusanuswerk*. TR is supported by the Hessian Ministry of Research and Art’s LOEWE initiative. The authors thank Esra Aslim for technical assistance in figure creation. Finally, the authors are grateful for the kind support provided by the *Verein zur Förderung der Epilepsieforschung e.V.* in Bonn.

## Author Contributions

CCP, BD, GS, BW, CEE, and TR contributed to the conception and design of the study. CCP, BD, JS, BW, RS, CEE, and TR contributed to the acquisition and analysis of data. All authors contributed to drafting the manuscript.

## Conflicts of Interest

None of the authors has any relevant conflict of interest with regard to current work to report.

## References

- Lemon RN. Descending pathways in motor control. *Annu Rev Neurosci.* 2008;31(1):195-218.
- Fawcett JW, Curt A. Damage control in the nervous system: rehabilitation in a plastic environment. *Nat Med.* 2009;15(7):735-736.
- Gaubatz J, Prillwitz CC, Ernst L, et al. Contralateral white matter alterations in patients after hemispherotomy. *Front Hum Neurosci.* 2020;14.
- Pascoal T, Paglioli E, Palmieri A, Menezes R, Staudt M. Immediate improvement of motor function after epilepsy surgery in congenital hemiparesis. *Epilepsia.* 2013;54(8):109-111.
- Bueteffisch CM. Role of the contralateral hemisphere in post-stroke recovery of upper extremity motor function. *Front Neurol.* 2015;6:214.
- Kuypers HGJM. Anatomy of the descending pathways. In: VB Brooks, ed. *Comprehensive Physiology*, pp. 597-666, 2010.
- Staudt M, Gerloff C, Grodd W, Holthausen H, Niemann G, Krägeloh-Mann I. Reorganization in congenital hemiparesis acquired at different gestational ages. *Ann Neurol.* 2004;56(6):854-863.
- Holloway V, Gadian DG, Vargha-Khadem F, Porter DA, Boyd SG, Connelly A. Reorganisation of sensorimotor function in children following vascular damage to the middle cerebral artery territory: an fMRI and somatosensory evoked potential study. *NeuroImage.* 2000;11(5):S138.
- Schulz R, Koch P, Zimmerman M, et al. Parietofrontal motor pathways and their association with motor function after stroke. *Brain.* 2015;138(7):1949-1960.
- Schulz R, Runge CG, Bönstrup M, et al. Prefrontal-premotor pathways and motor output in well-recovered stroke patients. *Front Neurol.* 2019;10:105.
- Wakamoto H, Eluvathingal TJ, Makki M, Juhasz C, Chugani HT. Diffusion tensor imaging of the corticospinal tract following cerebral hemispherectomy. *J Child Neurol.* 2006;21(7):566-571.
- Küpper H, Kudernatsch M, Pieper T, et al. Predicting hand function after hemidisconnection. *Brain.* 2016;139(9):2456-2468.
- Nelles M, Urbach H, Sassen R, et al. Functional hemispherectomy: postoperative motor state and correlation to preoperative DTI. *Neuroradiology.* 2015;57(11):1093-1102.
- Gaubatz J, Ernst L, Prillwitz CC, et al. Pyramidal tract and alternate motor fibers complementarily mediate motor compensation in patients after hemispherotomy. *Sci Rep.* 2020;10(1):1-11.
- Ward N. Assessment of cortical reorganisation for hand function after stroke. *J Physiol.* 2011;589(23):5625-5632.
- Lawrence DG, Kuypers HGJM. The functional organization of the motor system in the monkey: I. The effects of bilateral pyramidal lesions. *Brain.* 1968;91(1):1-14.
- Z'Graggen WJ, Fouad K, Raineteau O, Metz GAS, Schwab ME, Kartje GL. Compensatory sprouting and impulse rerouting after unilateral pyramidal tract lesion in neonatal rats. *J Neurosci.* 2000;20(17):6561-6569.
- Schieber MH, Schieber MH. The journal of physiology dissociating motor cortex from the motor. *J Physiol.* 2011;589:5613-5624.
- Honeycutt CF, Kharouta M, Perreault EJ. Evidence for reticulospinal contributions to coordinated finger movements in humans. *J Neurophysiol.* 2013;110(7):1476-1483.
- Ruber T, Schlaug G, Lindenberg R. Compensatory role of the cortico-rubro-spinal tract in motor recovery after stroke. *Neurology.* 2012;79(6):515-522.
- Schulz R, Park E, Lee J, et al. Synergistic but independent: the role of corticospinal and alternate motor fibers for residual motor output after stroke. *NeuroImage Clin.* 2017;15:118-124.
- Kulikova SP, Nikulin VV, Dobrynina LA, Nazarova MA. A possible sensory interpretation of alternate motor fibers relating to structural reserve during stroke recovery. *Front Neurol.* 2017;8:355.
- Canedo A. Primary motor cortex influences on the descending and ascending systems. *Prog Neurobiol.* 1997;51(3):287-335.
- Schramm J, Kral T, Clusmann H. Transylvian keyhole functional hemispherectomy. *Neurosurgery.* 2001;49(4):891-901.
- Fugl-Meyer AR, Jääskö L, Leyman I, et al. The post-stroke hemiplegic patient. 1. a method for evaluation of physical performance. *Scand J Rehabil Med.* 1975;7(1):13-31.
- Glasser MF, Sotiropoulos SN, Wilson JA, et al. The minimal preprocessing pipelines for the human connectome project. *NeuroImage.* 2013;80:105-124.
- Smith SM, Jenkinson M, Woolrich MW, et al. Advances in functional and structural MR image analysis and implementation as FSL. *NeuroImage.* 2004;23:S208-S219.
- Fischl B, Sereno MI, Dale AM. Cortical surface-based analysis: II. Inflation, flattening, and a surface-based coordinate system. *NeuroImage.* 1999;9(2):195-207.
- Greve DN, Van der Haegen L, Cai Q, et al. A surface-based analysis of language lateralization and cortical asymmetry. *J Cogn Neurosci.* 2013;25(9):1477-1492.

30. Pierpaoli C, Walke L, Irfanoglu M, et al. TORTOISE: an integrated software package for processing of diffusion MRI data. In: ISMRM 18th Annual Meeting. Stockholm; 2010:1597.
31. Griffanti L, Douaud G, Bijsterbosch J, et al. Hand classification of fMRI ICA noise components. *NeuroImage*. 2017;154:188-205.
32. Winkler AM, Ridgway GR, Douaud G, Nichols TE, Smith SM. Faster permutation inference in brain imaging. *NeuroImage*. 2016;141:502-516.
33. Salimi-Khorshidi G, Smith SM, Nichols TE. New approaches for nonstationary cluster-size and TFCE inferences. *NeuroImage*. 2009;47:S58.
34. Zalesky A, Fornito A, Bullmore ET. Network-based statistic: identifying differences in brain networks. *NeuroImage*. 2010;53(4):1197-1207.
35. Hayasaka S, Nichols TE. Combining voxel intensity and cluster extent with permutation test framework. *NeuroImage*. 2004;23(1):54-63.
36. Behrens T, Berg HJ, Jbabdi S, Rushworth MFS, Woolrich MW. Probabilistic diffusion tractography with multiple fibre orientations: what can we gain? *NeuroImage*. 2007;34(1):144-155.
37. Benecke R, Meyer BU, Freund HJ. Reorganisation of descending motor pathways in patients after hemispherectomy and severe hemispheric lesions demonstrated by magnetic brain stimulation. *Exp Brain Res*. 1991;83(2):419-426.
38. Staudt M. Brain plasticity following early life brain injury: insights from neuroimaging. *Semin Perinatol*. 2010;34(1):87-92.
39. Varadkar S, Bien CG, Kruse CA, et al. Rasmussen's encephalitis: clinical features, pathobiology, and treatment advances. *Lancet Neurol*. 2014;13(2):195-205.
40. Bernhardt J, Hayward KS, Kwakkel G, et al. Agreed definitions and a shared vision for new standards in stroke recovery research: the stroke recovery and rehabilitation roundtable taskforce. *Int J Stroke*. 2017;12(5):444-450.
41. Ward NS, Newton JM, Swayne OBC, et al. The relationship between brain activity and peak grip force is modulated by corticospinal system integrity after subcortical stroke. *Eur J Neurosci*. 2007;25(6):1865-1873.
42. Habas C, Cabanis EA. Cortical projection to the human red nucleus: complementary results with probabilistic tractography at 3 T. *Neuroradiology*. 2007;49(9):777-784.
43. Kumar S, Schlaug G. Enhancing swallowing recovery after a stroke by harnessing its bihemispheric organization. *Ann Neurol*. 2018;83(4):658-660.
44. Schlaug G. Even when right is all that's left: there are still more options for recovery from aphasia. *Ann Neurol*. 2018;83(4):661-663.
45. Edelman GM, Gally JA. Degeneracy and complexity in biological systems. *Proc Natl Acad Sci*. 2001;98(24):13763-13768.
46. Jones TA, Adkins DL. Motor system reorganization after stroke: stimulating and training toward perfection. *Physiology*. 2015;30(5):358-370.
47. Benowitz LI, Carmichael ST. Promoting axonal rewiring to improve outcome after stroke. *Neurobiol Dis* 2010;37(2):259-266.
48. Nirkko AC, Ozdoba C, Redmond SM, et al. Different ipsilateral representations for distal and proximal movements in the sensorimotor cortex: activation and deactivation patterns. *NeuroImage*. 2001;13(5):825-835.
49. Héту S, Grégoire M, Saimpont A, et al. The neural network of motor imagery: an ALE meta-analysis. *Neurosci Biobehav Rev*. 2013;37(5):930-949.